Figure 1A

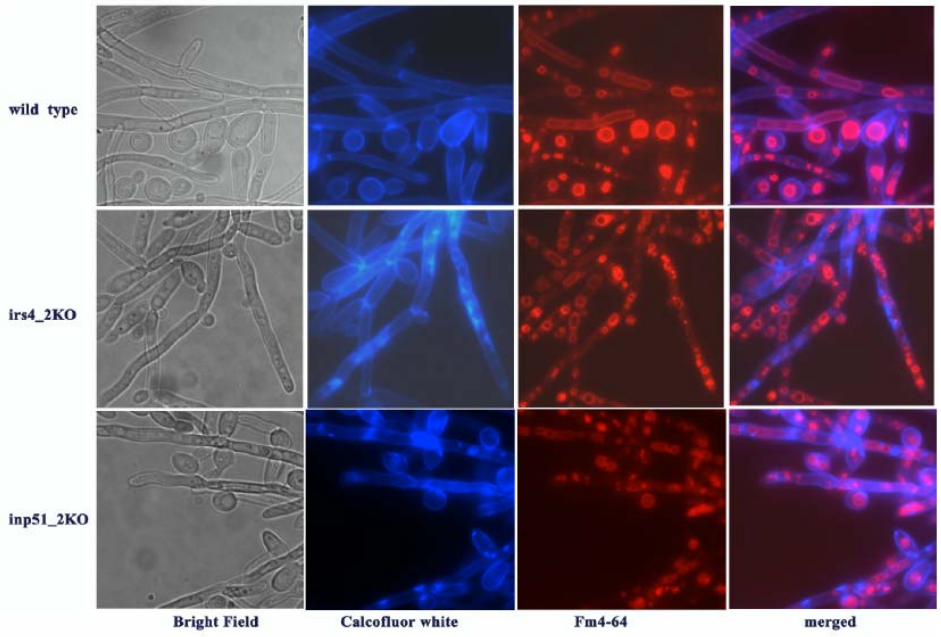

Figure 1B

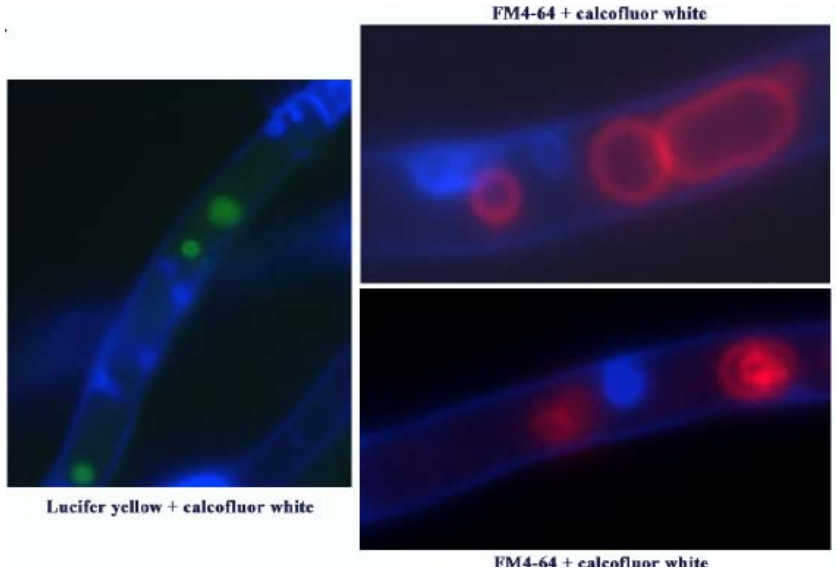

Supplemental figure 1. The aberrant chitin-containing structures in *irs4* and *inp51* mutants are distinct from endocytic vesicles. Wild-type, *irs4* and *inp51* cells grown were stained with calcofluour white to asses chitin distribution and FM4-64 or Lucifer yellow to assess endocytosis (Supplemental figure 1A). Calcofluor white localized to aberrant sites in mutant cells, but not wild-type cells. Staining with FM4-64 or Lucifer yellow revealed no differences in endocytosis between the mutant and wild-type strains. Overlay of images indicated a clear distinction between the calcofluour white-staining and FM4-64 or Lucifer yellow-staining structures. Higher resolution images mutant cells demonstrated clear distinction between chitin-containing structures (blue) and endocytic vesicles (FM4-64 staining is red; Lucifer yellow staining is green) (Supplemental figure 1B).

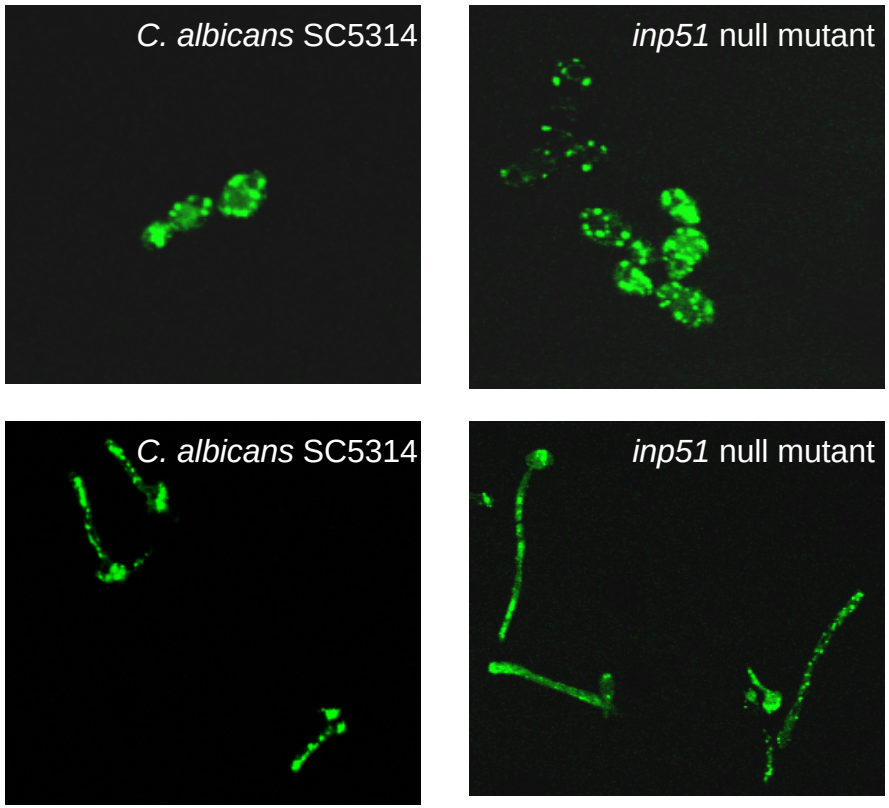

Supplemental figure 2. Vrg4-GFP distribution is normal in *irs4* and *inp51* mutant cells. Cells expressing a GFP-Vrg4 fusion were grown to induce hyphae at 37°C in YPD+5%FCS on the surface of glass-bottom culture dishes (MatTek, Ashland, MA) coated with Cell-Tak (BD Bioscience, Bedford, MA). All cells show normal Golgi structures. Cells were also fixed with 2% formaldehyde and stained with calcofluor white. The aberrant calcofluour white-straining structures in both *irs4* and *inp51* mutants do not co-localize with the GFP signal. Distribution of GFP-Arf1, GFP-Arf2, GFP-Rbt5 secretory signal and GFP-Sap1 secretory signal were also normal in mutant cells, and calcofluor white did not localize with GFP (images not shown).

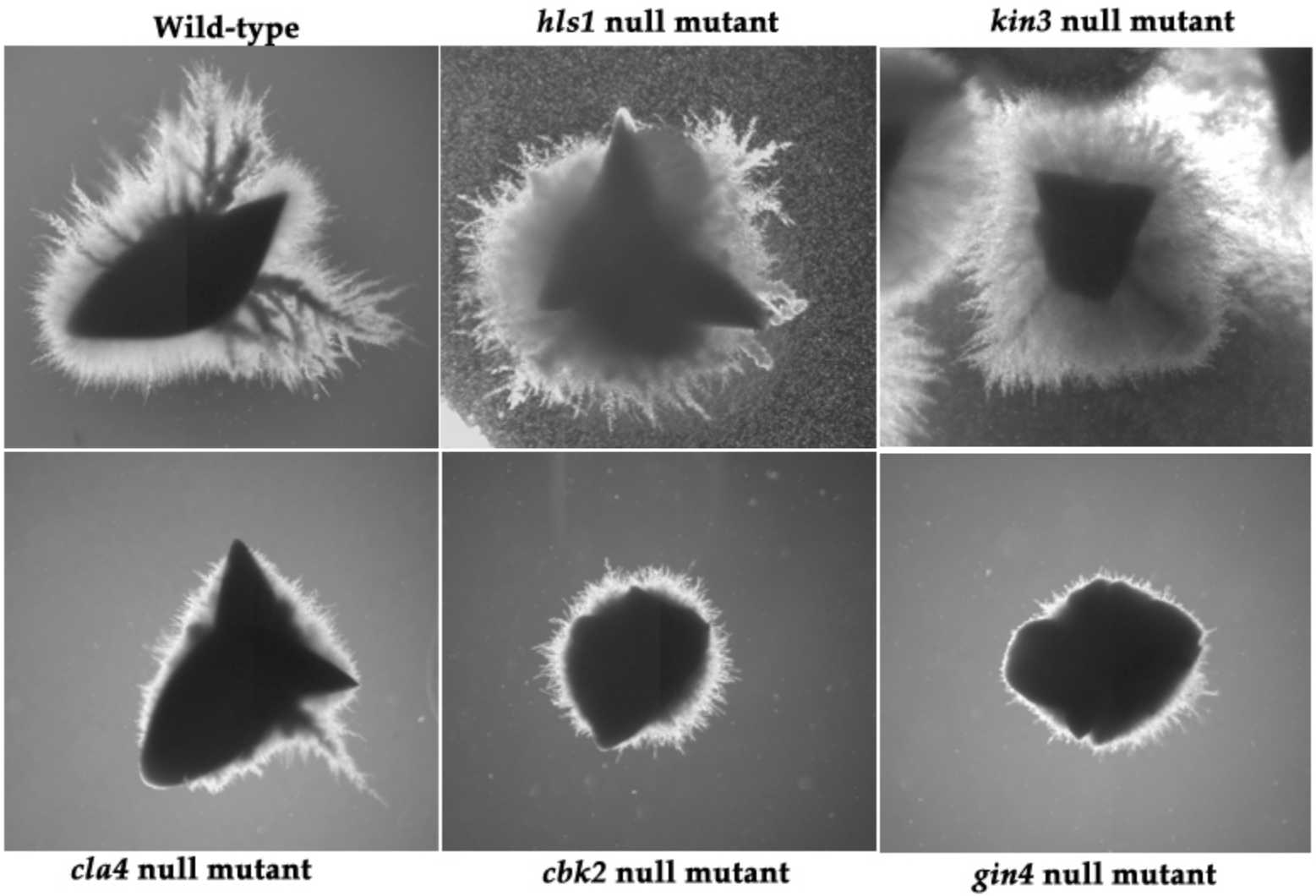

Supplemental figure 3a

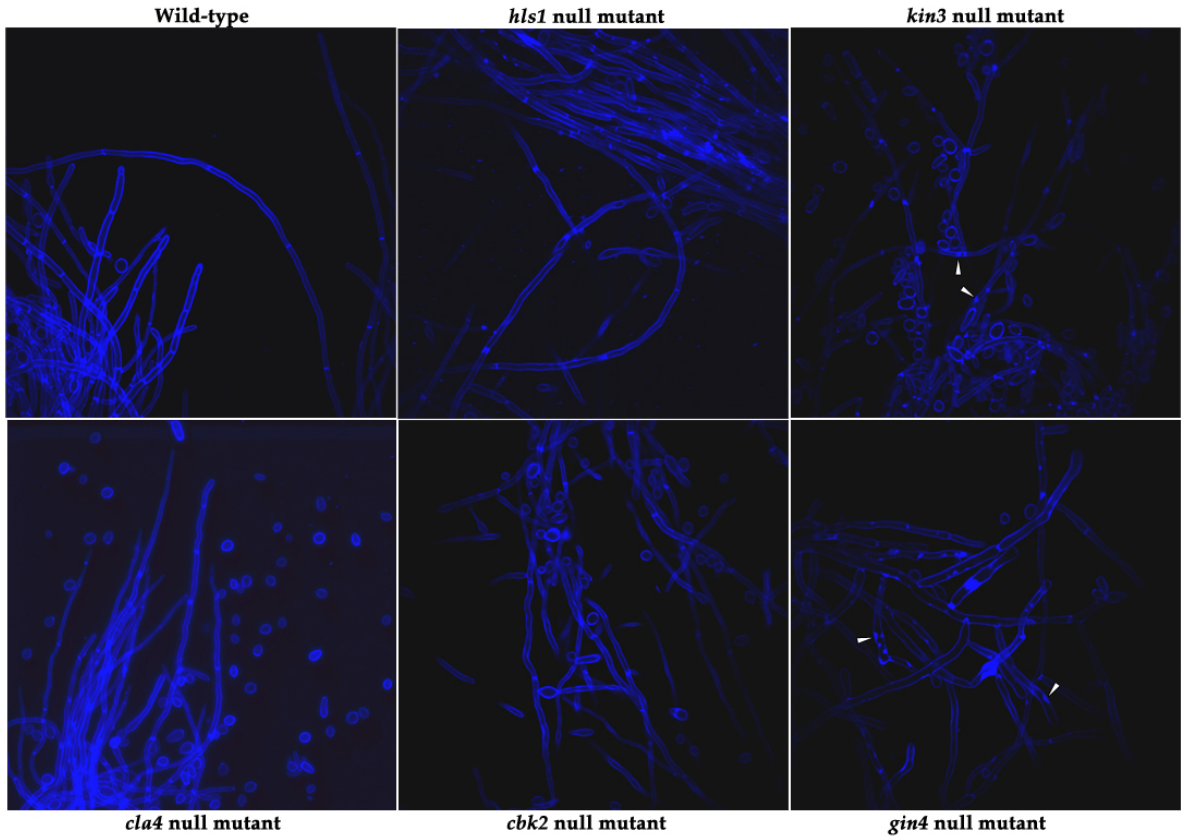

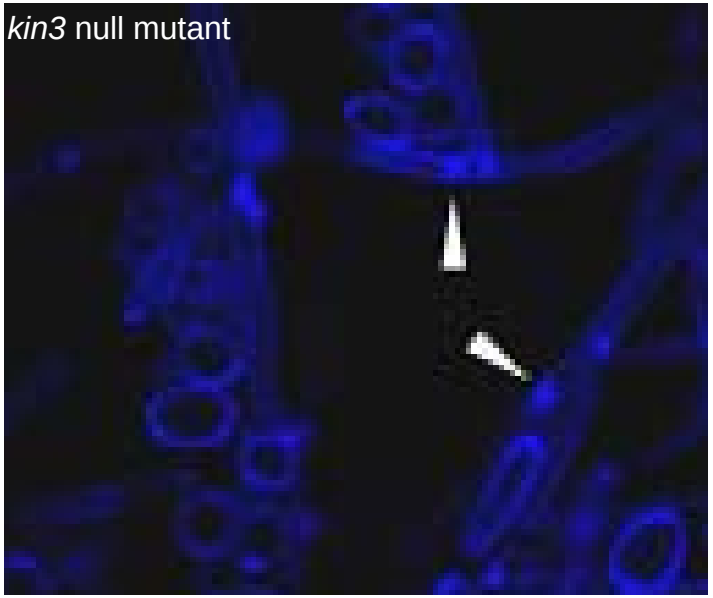

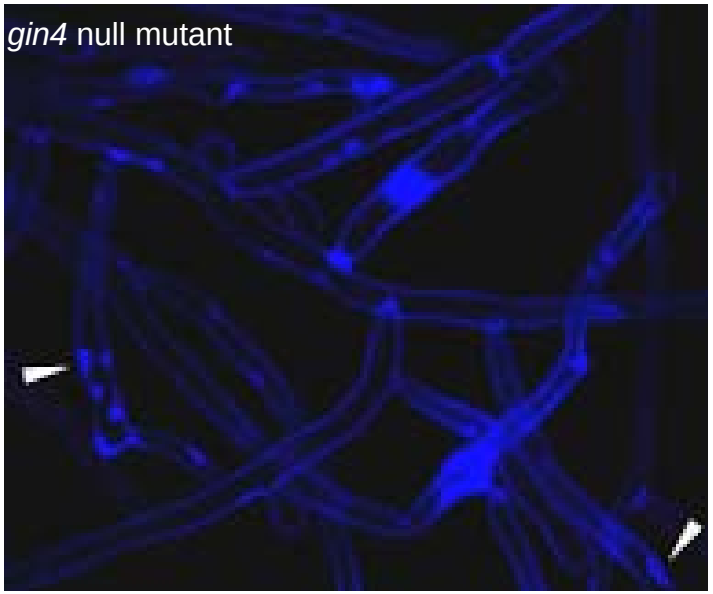

Supplemental figure 3b

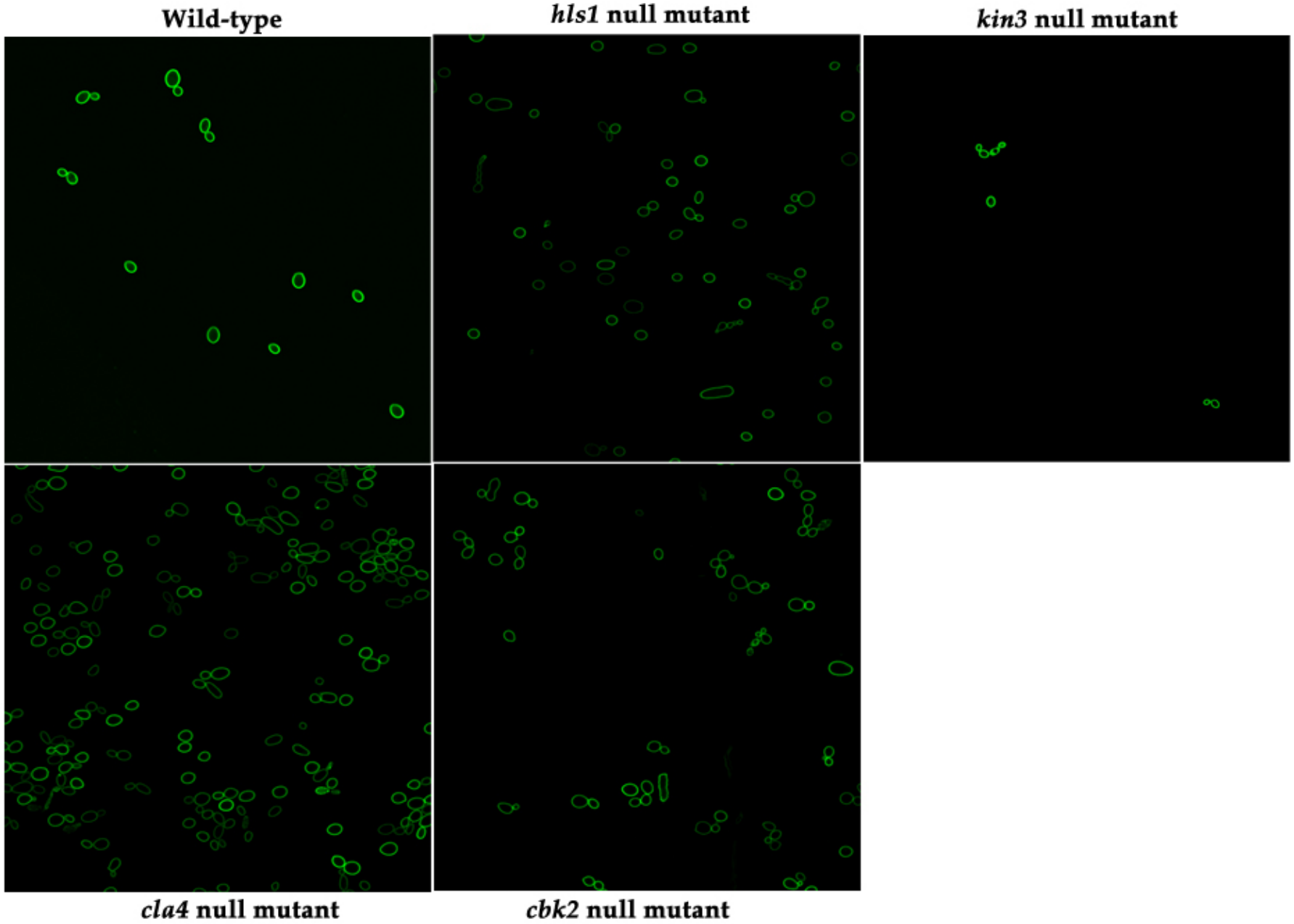

Supplemental figure 3c

Supplemental figure 3. Phenotypes of the *gin4* mutant most closely resemble *irs4* and *inp51* mutants. Invasive growth into agar (Supplemental figure 3A), calcofluour white localization (Supplemental figure 3B) and CaPH-GFP localization (Figure 3C) are shown for *hls1, kin3, cla4, ckb2* and *gin4* mutants. The phenotypes of mutants are summarized in Table 2. The *gin4* mutant resembled *irs4* and *inp51* in all phenotypes, consistent with the close relationship evident by gene expression profiling (see Figure 7). All phenotypes were identical for *gin4* mutants created in our original study, and in the present study using the SAT-flipper method. For all mutants, complementation of disrupted genes corrected aberrant phenotypes.